Particle trapping and self-focusing in temporally asymmetric ratchets with strong field gradients

Maurice J. Chacron and Gary W. Slater*
Department of Physics, University of Ottawa, 150 Louis-Pasteur, Ottawa, Canada K1N 6N5
(Received 10 February 1997)

We study the dynamics of a particle whose velocity is a nonlinear, monotonically increasing function of the applied field. The particle moves in a strong field gradient whose intensity and sign vary periodically. We demonstrate that if the field pulses are temporally asymmetric and biased, we can have situations where the particle always migrates towards a stable zero-velocity point. This special ratchet process can in principle be used to separate molecules and particles. An example is given for the electrophoresis of DNA. [S1063-651X(97)08509-7]

PACS number(s): 87.22.Fy, 82.45.+z, 05.40.+j, 05.60.+w

I. INTRODUCTION

As recently demonstrated by Magnasco [1], *ratchet potentials* (i.e., spatially asymmetric potentials) can rectify zero-mean correlated fluctuations and generate net motion. Temporally asymmetric, zero-mean fluctuations can also operate a correlation ratchet even when the potential is *spatially symmetric* [2,3]. Although one can design separation schemes (e.g., for charged particles) based on correlation ratchets, such systems provide limited resolution because the randomness of the ratchet transitions leads to a large overlap between the particle populations. Here we investigate a temporally asymmetric ratchetlike system that uses a small bias and a strong field gradient to make particles move towards attractor points where their velocity is zero. The particles then form self-focusing, well-separated zones. The principle is quite general and can be applied to different spatially symmetric ratchet potentials. The basic theoretical idea is introduced in Sec. II. As an example, we study, in Sec. III, a (one-dimensional) model of DNA gel electrophoresis for which exact solutions can be obtained. Other simple systems can also be treated easily.

II. BASIC PRINCIPLES OF THE METHOD

The instantaneous velocity $V(M,E)$ of a particle of size (e.g., charge) M in a local field of intensity E (e.g., an electric field) can be written as the product of E and the mobility $\mu(M,E)$,

$$V(M,E) \equiv \mu(M,E)E = \mu_0 E \times \mu^*(M,E), \qquad (1)$$

where μ_0 is some standard mobility and $\mu^*(M,E)=\mu/\mu_0$ is the reduced (or dimensionless) mobility. The system is nonlinear if μ^* is field dependent (μ^* is assumed to increase monotonically with E). Whatever the source of this nonlinearity, one can use such a system to build a correlation ratchet that rectifies temporally biased fluctuations, as described in [2]. Nonlinearities often diminish the resolution of separation processes. Here, however, we will exploit them.

*Author to whom correspondence should be addressed. Electronic address: gary@physics.uottawa.ca

Let us first discuss a simple ac process where the field is E_0 in the forward direction and E_0/R_E in the reverse direction (there is no field gradient for the moment), while the pulse durations are T_0 and $R_T T_0$, respectively, with $R_E>1$ and $R_T>1$ [Fig. 1(a)]. Although the mean-field intensity is zero for $R_T=R_E$, we then have a net velocity $V_n>0$ if the system is nonlinear [3]. This is essentially the idea behind the temporal ratchet of Ref. [2] and the so-called zero-integrated-field-electrophoresis process [4]. Here, instead, we choose $R_T>R_E>1$ (a negative bias). Since the mobility increases with the field intensity E, it is possible to find ratios R_T and R_E such that we have $V_n(E_0\to 0)<0$ (the bias dominates the nonlinearity) while $V_n(E_0\to\infty)>0$ (the nonlinearity dominates the bias). This implies the existence of a finite critical field $E_0=E^*(M)$ for which $V_n(M)$ is exactly zero. Under these conditions, the particle will simply oscillate around a fixed position in response to the biased ac external field. Now, if this process is carried out in a field gradient, a particle of size M will naturally move towards the point where the local field intensity

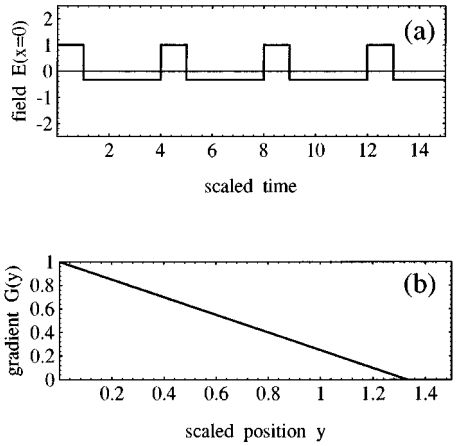

FIG. 1. (a) Schematic of the field (square) pulses used here (in dimensionless units). The field intensity is R_E times larger in the positive direction, but the pulse duration is R_T times longer in the negative direction (for this figure $R_E=R_T=3$). (b) Field gradient function $G(y)$ used for our calculation. The function G decreases linearly from unity at $y=0$. The point $y=y_\nabla$, where $G=0$ is situated outside the system, which is limited to $0<y<1$. For this figure $y_\nabla=\frac{4}{3}$.

$E(x)$ is equal to its own critical field $E^*(M)$. After reaching this position, it will have a zero net velocity and will just oscillate around this point in response to the applied pulses. Since the particle will move towards this ''attractor'' point from either side of it, the distribution of particles of size M will self-sharpen as a function of time. The situation is, in fact, similar to protein isoelectrofocusing [5]. Since particles with different sizes M will generally stop at different positions in the system, our ''isofocusing-ratchet'' can separate particles.

In order to establish the basic equations describing the conditions that are necessary for such a self-focusing ratchet to work, let us examine a simple one-dimensional separation system defined from $x=0$ to L. The field $E(x,t)$, at a position x and at a given time t, is given by

$$E(x,t)=E_i(t)G(x/x_\nabla), \tag{2}$$

where $E_i(t)=E(0,t)$ is the intensity at the $x=0$ end of the system and x_∇ is a length describing the strength of the field gradient. The function $G(z)$, which satisfies $G(0)=1$ and $1\geqslant G(L/x_\nabla)>0$, is assumed to be a monotonically decreasing function of its argument (nonmonotonic functions will be discussed in Sec. IV). The field $E_i(t)$ varies as shown in Fig. 1(a): Its intensity is $E_i(t)=E_0$ for a time duration T_0, followed by $E_i(t)=-E_0/R_E$ for a duration $R_T T_0$. The period is $T_0(R_T+1)$ and the mean field intensity is $\langle E\rangle=E_0(1-R_T/R_E)/(1+R_T)$. Note that the mean-field intensity is zero if $R_T=R_E$.

Let us assume for a moment that T_0 is short enough that we can neglect the change of local field intensity felt by the particle during a complete pulse. The distance migrated by a particle during a positive pulse is then $V(M,E)T_0$, while the distance migrated during the following negative pulse is $-V(M,E/R_E)R_T T_0$. We have a fixed point when the local field $E(x)$ is such that these two displacements exactly cancel one another. The equation for the position x_{if} of the fixed point is thus

$$\frac{\mu^*(M,E(x_{if}))}{\mu^*(M,E(x_{if})/R_E)}=\frac{R_T}{R_E}. \tag{3}$$

Since the mobility μ^* is an increasing function of the field intensity, the left-hand side is larger than unity. A fixed point thus exists only if $R_T>R_E$, i.e., if the ratchet is biased in the negative direction, as expected. If the particle at position $x(t)$ is moving towards $x_{if}(M)$, the equation of motion describing its displacement during a complete cycle is (for T_0 small)

$$dx/dt\approx[V(M,E(x))-R_T V(M,E(x)/R_E)]/(1+R_T). \tag{4}$$

It is easy to see from Eqs. (3) and (4) that $dx/dt>0$ if $x<x_{if}$, while $dx/dt<0$ if $x>x_{if}$. Therefore, the fixed point acts like an attractor for the particle. The argument presented above is valid only if $T_0\ll E/V\nabla E$, i.e., for very short pulses. For finite pulse durations, the particle will ultimately oscillate between two positions, which we will denote x_i and x_f, with the distance $\Delta x_{if}=x_f-x_i$ between these positions getting smaller as T_0 decreases. The fixed point is located between these two points ($x_i\leqslant x_{if}\leqslant x_f$) and both x_i and x_f converge towards x_{if} when $T_0\to 0$.

The ideas presented in this section are quite general and can be applied to a wide range of systems characterized by a nonlinear, monotonically increasing mobility. Given a potential $G(x/x_\nabla)$ and a nonlinear mobility $\mu^*(M)$, we can solve Eqs. (3) and (4) for the position $x(t)$, the final position $x_{if}(M)$, the final width $\Delta x_{if}(T_0)$, and finally the migration time necessary to reach the fixed point $x=x_{if}$. When the function $\mu^*(M,E)$ is sufficiently simple, exact solutions can be obtained (this is the case for the example solved in the next section). Otherwise, one must rely on numerical solutions.

III. AN EXAMPLE WITH AN EXACT SOLUTION: DNA GEL ELECTROPHORESIS

Gel electrophoresis is one of the most important laboratory technique in modern molecular biology [4–8]. For example, it is used both to map and sequence the genome of living organisms. DNA fragments are highly charged in aqueous buffers and thus readily migrate through dense gels in response to external electric fields. The sieving effect of the gel often provides high-resolution separations of mixtures of fragments, although there are severe limitations in some cases (e.g., for very large DNA fragments and/or high fields). The field and molecular size dependence of the dc gel electrophoretic mobility of a DNA fragment is well described by the simple relationship [6–8]

$$\mu^*(M,E)=\frac{M_a}{M}+\left|\frac{E}{E_a}\right| \quad \text{for } E<E_a, \quad M>M_a, \tag{5}$$

where M_a and E_a are fitting constants. Another relationship has recently been suggested [8]; although it reduces to Eq. (5) in both the low- and high-field limits, it would not allow us to obtain exact results. Other empirical models can be used instead of Eq. (5) without affecting the general (qualitative) results of our study. We will also use a simple linear gradient

$$G\left(\frac{x}{x_\nabla}\right)=1-\frac{x}{x_\nabla} \quad \text{with } 0\leqslant x\leqslant L<x_\nabla \tag{6}$$

in order to obtain analytical results [Fig. 1(b)]. We now switch to dimensionless variables for the rest of this paper. We will use the system size L as a unit of length and $t_L=L/\mu_0 E_0$ as a unit of time; the new variables are thus $\varepsilon=E_0/E_a$, $m=M/M_a$, $y=x/L$, $\tau=t/t_L$, $\tau_0=T_0/t_L$, and $y_\nabla=x_\nabla/L$.

Solving Eqs. (3), (5), and (6) for the equilibrium position $y_{if}(m)$, we find

$$y_{if}(m)=y_\nabla\left(1-\frac{m^*}{m}\right), \tag{7}$$

where the critical molecular size m^* is given by

$$m^*=\frac{R_T/R_E-1}{\varepsilon(1-R_T/R_E^2)}. \tag{8}$$

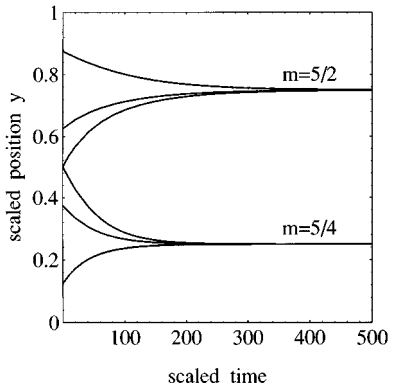

FIG. 2. Trajectories followed by three $m=\frac{5}{2}$ and three $m=\frac{5}{4}$ particles. The conditions are $R_E=1+\sqrt{2}$, $R_T=11(R_E)^2/(2+9R_E)=2.70$, $y_\nabla=\frac{5}{4}$, and $\varepsilon=\frac{2}{9}$. Six initial positions were used. The attractors are at $y_{if}=\frac{1}{4}$ and $\frac{3}{4}$ for these conditions.

The molecules thus indeed reach different positions along the system. Since we must have $0<y_{if}<1$, the range of molecular sizes that can be separated is restricted to $m^*<m<m^*/(1-1/y_\nabla)$. Smaller (larger) molecules move beyond $y<0$ (or $y>0$) and are thus lost. The range of sizes that is separated is large if the gradient width y_∇ is close to unity, but may be quite narrow for weaker gradients. In order to ensure that $m^*>0$, the bias must actually be limited by the relationship

$$R_E^2>R_T>R_E. \tag{9}$$

It is also easy to solve Eq. (4) for the linear field gradient and the mobility relation (5). Using Eq. (7), we can write the position $y(m,\tau)$ at time τ as

$$\frac{y(m,\tau)-y_{if}(m)}{y_0-y_{if}(m)}=\left[1+\left(\frac{y_\nabla-y_0}{y_\nabla-y_{if}}\right)[\exp(\tau/\tau_m)-1]\right]^{-1}, \tag{10}$$

where $y_0=y(m,\tau=0)$ is the initial position of the particle. The characteristic time τ_m is given by

$$\tau_m=my_\nabla R_E\left(\frac{R_T+1}{R_T-R_E}\right). \tag{11}$$

The distance $y(\tau)-y_{if}$ to the fixed point thus decreases exponentially with time. Figure 2 shows some trajectories for six initial positions y_0 and two molecular sizes m. Clearly, we see two attractors, one for each particle size. Also, the relaxation time increases (linearly) with size m.

Rewriting Eq. (4) for small values of the distance $Y(\tau)=y(m,\tau)-y_{if}(m)$ to the attractor, we find the equation of motion $dY/d\tau=-Y/\tau_Y$ for the final approach, with $\tau_Y=\tau_m/(1-y_{if}/y_\nabla)\propto y_\nabla/\varepsilon$. This is the equation for the motion for a particle attached to a linear spring and moving in a very viscuous fluid; the spring constant is $K_Y\propto\varepsilon/y_\nabla$. The point $y=y_{if}$ is thus stable and τ_m is a good measure of the time necessary to reach it. A sharper gradient and a higher-field intensity are predicted to lead to faster self-focusing dynamics. Note, however, that the ultimate ($\tau\to\infty$) width of the population will not be zero because the diffusion processes (which we have neglected) will lead to a finite band width $\sim(D/K_Y)^{1/2}$, where D is the diffusion coefficient of the particles. We will not study this any further because we would need a specific high-field model for $D(\varepsilon)$; moreover, as we will see next, the fact that the (scaled) pulse duration τ_0 has to be finite also imposes a finite width to the final distribution of particles.

The previous discussion is valid only for infinitely short pulse durations ($T_0\to0$). In practice, we cannot reduce T_0 below a certain threshold due to the transient effects one would expect following a sudden change in field direction. Indeed, the theory presented so far assumed that T_0 is long enough for the steady-state mobility $\mu^*(M,E)$ to be the relevant mobility during (almost all of) the pulse. Therefore, we must examine the dynamics over a complete cycle for finite pulse durations.

The equation of motion for a positive pulse ($E_i=E_0$) is $dy/d\tau=[1/m+\varepsilon G(y/y_\nabla)]G(y/y_\nabla)$; it is easy to solve this equation over the duration τ_0 of the forward pulse and between the initial and final positions y_i and y_f in order to obtain the new position $y_f(y_i,\tau_0,m,\varepsilon)$. Similarly, one can establish and solve the equation of motion for the following backward pulse during which the particle migrates from $y=y_f$ towards the final position $y=y_p$ in a time $R_T\tau_0$; this gives us the new position $y_p(y_f,R_T\tau_0,m,\varepsilon/R_E)$. The net displacement during a complete cycle is y_p-y_i and the steady state is obviously reached when $y_i=y_p$. If we solve these equations for y_i and y_f with the condition $y_i=y_p$, we find that in the steady state, the particle oscillates between the positions

$$y_{fss}=y_{if}+\frac{R_E^2(R_E-1)(R_Th_2/R_E-h_1-1)}{\varepsilon m(R_E^2-R_T)(R_Eh_2-h_1-1)}y_\nabla\approx y_{if}+\frac{\tau_0}{2\tau_c}+O(\tau_0^2) \tag{12}$$

and

$$y_{iss}=y_{if}-\frac{R_E^2(R_E-1)(1-R_T(h_2-h_1)/R_E)}{\varepsilon m(R_E^2-R_T)[R_E(h_2-h_1)-1]}y_\nabla\approx y_{if}-\frac{\tau_0}{2\tau_c}+O(\tau_0^2), \tag{13}$$

where $h_1=\exp(\tau_0/my_\nabla)-1$, $h_2=h_1/[1-\exp(-R_T\tau_0/R_Emy_\nabla)]$, and the critical pulse duration τ_c is given by

$$\tau_c=\frac{\varepsilon m^2(R_E^2-R_T)^2}{R_ER_T(R_E-1)(R_T-R_E)}. \tag{14}$$

As can be verified, we have $y_{fss}\geqslant y_{if}\geqslant y_{iss}$, with the equality signs holding for $\tau_0\to0$. To first order in τ_0, the ideal fixed point y_{if} is in fact exactly between the points y_{iss} and y_{fss}.

In Fig. 3 we show the positions $y(\tau)$ of the particle at the end of each pulse (both positive and negative) for $\tau_0=0.1$, $y_0=0$, $m=\frac{15}{8}$, and the parameters used for Fig. 2 [the inset shows the complete $y(\tau)$ vs τ curve for the first three cycles]. We see two well-separated lines with the ideal solution (10) situated between them. The relaxation time is identical for all three curves, indicating that Eq. (11) is also useful for finite pulse durations. From Eqs. (12) and (13) the apparent spatial width $\Delta y=y_{fss}-y_{iss}$ of these oscillations is

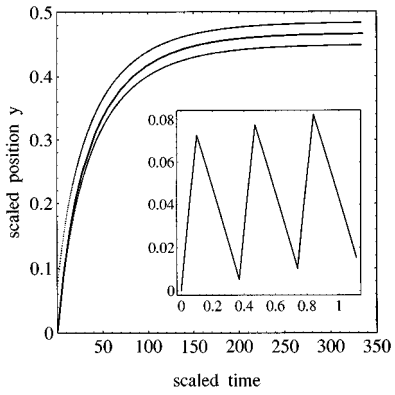

FIG. 3. Dynamics of an $m=\frac{15}{8}$ particle, starting at $y_0=0$, with the pulse duration $\tau_0=0.1$. The other conditions are as given in Fig. 2. The middle curve gives the behavior for $\tau_0\to 0$, while the two dashed lines give the positions of the particle at the end of each pulse. Inset: zoom on the trajectory for the first three pulses.

given by $\Delta y\approx\tau_0/\tau_c\propto\tau_0/\varepsilon m^2$. Shorter pulses, larger field intensities, and larger molecular sizes all favor narrower bands; the strength of the gradient (y_∇), however, does not appear in this relation. In practice, if a certain width Δy is required experimentally, $\tau_0=\tau_c\Delta y$ gives the pulse duration to use (as long as τ_0 remains long compared to the duration of the transients); moreover, one can calculate the required separation time $\tau_{\rm expt}$ by solving Eq. (10) for $|y(m,\tau_{\rm expt})-y_{if}(m)|=\Delta y$ [indeed, there is no point in getting closer than Δy to the fixed point $y_{if}(m)$].

In practice, the shape of the gradient function $G(y)$ can be chosen to lead to any desired final distribution $y_{if}(m)$. For example, a linear distribution of the form $y_{if}(m)\sim 1-m/m^*$ can be obtained for the mobility function given by Eq. (5) if we use a hyperbolic function of the type $G(z)=1/(1+z)$ instead of Eq. (6). Also, very sharp gradients can lead to very narrow bands and extremely high resolution for wide ranges of particle sizes, while weak gradients lead to the separation of very narrow ranges of sizes (at the cost of having broader bands). This would be particularly useful in molecular biology where gel electrophoresis is frequently used to estimate DNA and protein molecular sizes and find minute size differences. In this case, the local electric field intensity is controlled by the local thickness of the gel, which makes it possible to design customized field gradients $G(y)$.

IV. DISCUSSION

We have demonstrated in Sec. II that it is possible to build an isofocusing type of ratchet using a strong field gradient, biased fluctuations, and a nonlinear system. As an illustrative example, we described the exact analytical solution for a DNA gel electrophoresis system (Sec. III). However, other systems can also be designed. For instance, one could also use Chialvo and Millonas's ratchet potentials or the entropic trapping (steric) potential of Ref. [3].

The gradient presented in Sec. III is not optimal and was chosen solely because it is simple enough that a complete analytical study can be presented. However, it is interesting to look at the practicality of the proposed DNA separation scheme. In order to minimize separation times, one must minimize the critical size m^*. Let us take $m^*=2$ for this discussion. This requires, from Eq. (8), that $R_T/R_E=R_E(2\varepsilon+1)/(2\varepsilon+R_E)$. With realistic values such as $R_E=\frac{5}{2}$ and $\varepsilon=\frac{1}{2}$, we then get $R_T=\frac{25}{7}$. Using $y_\nabla=\frac{5}{4}$, which ensures that molecules in the range $2<m<10$ get separated on the gel, Eq. (11) yields $\tau_m\approx 5m$. The migration time of a $m=m^*=2$ molecule in the absence of pulsed fields and gradients being $L/V\approx 1$ in our scaled units, this represents a fivefold increase in separation time for the smaller size (and a threefold increase for $m=10$), a result that appears interesting in practice if the system provides improved resolution. In order to reduce separation time, one could load the gel in the middle or first apply a dc field in order to bring the molecules close to their expected final positions. The result would be quite unique: The $m=2-10$ molecules would be spread over the entire gel. If the gel is long, this may provide superb resolution over that size range. For an agarose gel, M_a is a few kilo base pairs (kbp) [8]; one could thus have the 5–25 kbp molecules spread over 20 cm of gel.

More complicated isofocusing ratchets can be built using more complicated gradients and/or mobility relationships. For instance, a gradient of the form $G(y/y_\nabla)=1+A\sin(\lambda y/y_\nabla)$ could have, for $0<A<1$ and $\lambda\gg 1$, multiple attractor points for each particle. Particles would thus be attracted to the nearest attractor. Similar behavior can also be expected if the mobility is not a monotonic function of the field intensity. In each case, a small difference in the initial position y_0 could lead to quite different final destinations. Very interesting situations can also occur if the system has a rough field landscape $G(y)$. We could then have numerous attractors and very complicated trajectories, especially for long pulse durations.

V. CONCLUSION

In conclusion, we have established the basic phenomenology of a separation process where nonlinear mobilities, strong field gradients, and biased asymmetric pulses lead to the existence of stable, zero-velocity points that act like attractors for the migrating particles. The process is somewhat reminiscent of protein isoelectric focusing; here, however, the existence of the zero-velocity points is solely due to dynamical reasons.

ACKNOWLEDGMENTS

The authors would like to thank Dr. Pascal Mayer for fruitful discussions. This work was supported by a Research Grant from the National Science and Engineering Research Council of Canada to G.W.S., and by financial support from the University of Ottawa to M.J.C.

[1] M. O. Magnasco, Phys. Rev. Lett. **71**, 1477 (1993).
[2] D. R. Chialvo and M. M. Millonas, Phys. Lett. A **209**, 26 (1995).
[3] G. W. Slater, H. L. Guo, and G. I. Nixon, Phys. Rev. Lett. **78**, 1170 (1997).
[4] C. Turmel, E. Brassard, R. Forsyth, K. Hood, G. W. Slater, and J. Noolandi, in *Electrophoresis of Large DNA Molecules—Theory and Applications*, edited by E. Lai and B. W. Birren (Cold Spring Harbor Laboratory Press, Plainview, NY, 1990), pp. 101–131.
[5] R. Westermeier, *Electrophoresis in Practice* (VCH, Weinheim, 1993).
[6] A. N. Semenov, T. A. J. Duke, and J.-L. Viovy, Phys. Rev. E **51**, 1520 (1995).
[7] L. Mitnik, L. Salomé, J.-L. Viovy, and C. Heller, J. Chromatogr. A **710**, 309 (1996).
[8] G. T. Barkema, C. Caron, and J. F. Marko, Biopolymers **38**, 665 (1996).